IEEE Access
Multidisciplinary | Rapid Review | Open Access Journal

Received July 18, 2020, accepted August 10, 2020, date of publication August 14, 2020, date of current version August 26, 2020.

Digital Object Identifier 10.1109/ACCESS.2020.3016783

Research on the Orthogonal Fundamental Mode Fluxgate Sensor Circuit

ZHENZHONG YUAN[1], YUXIN ZHANG[1], DONG WANG[1], YINGDAN JIANG[1], AND RONGHAI GUO[2]

[1]China Electronics Technology Group Corporation No. 58 Research Institute, Wuxi, China
[2]Military Representative Office of the Army in Nanchang, Nanchang, China

Corresponding author: Zhenzhong Yuan (yngsky@yeah.net)

ABSTRACT Currently, magnetic fluxgate circuits used for magnetic field measurements mostly adopt parallel excitation second harmonic generation. The magnetic fluxgate developed by this method cannot possess both low noise and high bandwidth at the same time. The orthogonal fundamental mode fluxgate is used in this paper: the excitation magnetic field is orthogonal to the magnetic field to be measured, and the external magnetic field is detected by measuring the voltage signal in the pick-up coil. The excitation magnetic field changes with the parallel excitation second harmonic method while the direction of the excitation magnetic field does not change in the orthogonal fundamental mode scheme, which can effectively reduce the influence of Barkhausen noise. The magnetic fluxgate circuit is designed based on the orthogonal fundamental mode scheme and its performance indexes are tested. The range of the magnetic fluxgate is $\pm$100000 nT, the sensitivity is 100 μV/nT, the output noise is 8.9 pT/rt(Hz)@1 Hz, and the bandwidth is DC-15 kHz. The orthogonal fundamental mode fluxgate improves the bandwidth performance while enabling low-noise magnetic field measurements in practical applications.

INDEX TERMS Low noise fluxgate, orthogonal fundamental mode, Barkhausen noise.

I. INTRODUCTION

Magnetic field detection equipment, geomagnetic navigators, nondestructive testing equipment, electromagnetic tracking devices and other magnetic measurement instruments and equipment are widely used in many fields such as scientific research, national economic construction (i.e., geology, industry, medical care), national defense construction, etc. As a common core part, a high-resolution triaxial weak magnetic sensor becomes the key to affecting the comprehensive performance of these instruments and equipment [1], [2]. In all the types of high-resolution triaxial weak magnetic sensors, fluxgate sensors can be used as the preferred component for magnetic field detection, electromagnetic tracking and other equipment applications due to their comprehensive performance advantages, i.e., their low noise, high sensitivity and small volume [3]–[6].

The parallel excitation second harmonic method is often used for the probe excitation of a fluxgate, and the Mag series of products of Bartington in England are relatively mature. A low-noise fluxgate has a noise of 10 pT/rt(Hz)@1 Hz, a bandwidth of 3 kHz, with a linearity error of 0.0015%. In 2002, I. Sasada *et al.* from Kyushu University in Japan designed a fluxgate prototype of the orthogonal fundamental mode, which effectively suppresses Barkhausen noise, the main noise source of the magnetic core, by using bias excitation. In 2004, E. Paperno from Ben-Gurion University in Israel reduced the noise to 10 pT/rt(Hz)@2 Hz by optimizing the excitation parameters [7]. In 2009, P.Ripka *et al.* of Czech Technical University designed an orthogonal excitation fluxgate with multiturn glass-coated amorphous wire magnetic core structure to improve sensor sensitivity. In 2013, I.Sasada *et al.* reduced the level of noise to 1.8 pT/rt(Hz)@1 Hz on 45 mm magnetic core structure by improving the annealing process of amorphous magnetic core material. In 2014, R.Bazinet *et al.* from Phoenix Geophysics in Canada designed an orthogonal fundamental mode fluxgate based on cobalt-based amorphous wire materials, reducing the amount of noise to 1.5 pT/rt(Hz)@1 Hz on a 25 mm magnetic core structure, and proposed a fluxgate digitization scheme. Judging from the new theoretical research, many scholars' research on the fluxgate of orthogonal fundamental

The associate editor coordinating the review of this manuscript and approving it for publication was Mohsin Jamil.

mode systems is still at the theoretical stage and no corresponding products have been developed. In 2018, Mattia Butta presented a method to reduce the low-frequency noise of an orthogonal fluxgate in fundamental mode, consisting of the application of a layer of silicone to the magnetic core, which in turn reduces the speed of variation in its temperature. This method can effectively reduce low frequency noise [8]–[11].

Many scholars have studied how to reduce the noise of the magnetic core, but have not combined the magnetic core and a circuit to form a magnetic field measurement product.

II. PRINCIPLE OF ORTHOGONAL FUNDAMENTAL MODE FLUXGATE

In the parallel excitation second harmonic method, the excitation coil and the induction coil are wound around an iron core made of soft magnetic material, as shown in Fig. 1. The signal generating the excitation magnetic field is generally a bipolar square wave signal, the excitation magnetic field is parallel to the magnetic field to be measured, and the external magnetic field is detected by measuring the second harmonic component in the output voltage of the induction coil [12].

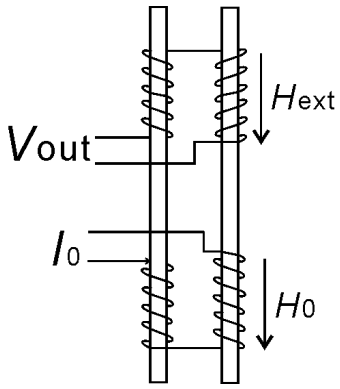

FIGURE 1. Structural diagram of the parallel excitation second harmonic method(H_{ext}: External magnetic field, V_{out}: Pick-up coil output voltage, I_0: Current formed by excitation voltage, H_0: Excitation magnetic field).

The structure of the orthogonal fundamental mode fluxgate sensor is shown in Fig. 2. The magnetic core of the sensor probe is a cobalt-based amorphous wire of $(Co_{0.94}Fe_{0.06})_{72.5}Si_{12.5}B_{15}$ with a diameter of 120 μm. When the amorphous wire is excited by an axial alternating magnetic field, its magnetic permeability can be changed by changing the external magnetic field, and it has high sensitivity. The longer the amorphous wire is, the higher the sensitivity and the lower the noise. The amorphous wire used in the design is 25 mm. The cobalt-based amorphous wire is coated with a glass layer outside, the wire is placed in a ceramic tube, enameled wires are wound around the outside of the tube, the diameter of the enameled wires is 0.12 mm, and 1200 turns of the enameled wires are wound. The output voltage of the induction coil carries the information of the magnetic field to be measured. The sensor probe is excited by an alternating current with bias, and the magnitude of the excitation current changes without changing the direction, thus effectively reducing the Barkhausen noise caused by the alternating magnetic field [13], [14].

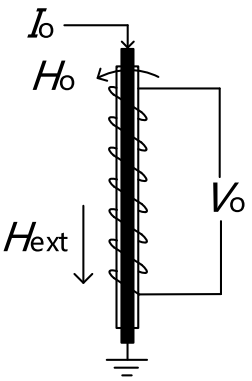

FIGURE 2. Orthogonal fundamental mode fluxgate sensor structure(I_o: Excitation current, V_o: Pick-up coil output voltage).

The amorphous wire after preparation is coated with a glass layer outside. A microphotograph of the amorphous wire after corrosion in HF solution is shown in Fig. 3. It can be seen that the diameter and appearance of the amorphous wire are very smooth and uniform except for some residual glass, and it is uniformly coated by the glass layer.

FIGURE 3. Microphotograph of corroded glass coating.

Before the amorphous wire is made into a sensor probe, a circumferential dynamic hysteresis loop of the core wire is created. The hysteresis loop, i.e., the magnetization curve, reflects the relationship between the magnetic flux density M and magnetic field strength H of a ferromagnetic material during magnetization. A block diagram of the test principle is shown in Fig. 4. The signal generator provides AC (alternating current) or DC (direct current) voltage. The red part in Fig. 4 is the location of the amorphous wire. R3 adjusts the balance of the Wheatstone bridge. The preamplifier amplifies

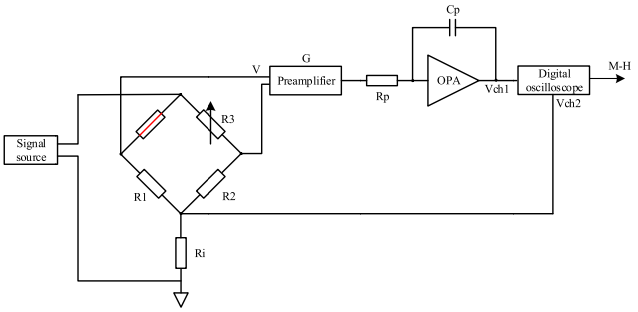

FIGURE 4. Circumferential dynamic hysteresis loop test circuit.

the voltage output at both ends of the Wheatstone bridge. The two output voltages are connected to both ch1 and ch2 of the digital oscilloscope to observe the Lissajous waveform.

The circuit consists of a bridge circuit, an RC integration circuit and a noninverting amplifier. The value of R1, R2, Ri is 49.9 Ω. Excessive resistance value will affect the excitation current stability. If the resistance value is too small, the signal-to-noise ratio of the bridge output voltage signal will be too bad, which will affect the test results. The time constant of the integrating circuit is determined by Rp (2 kΩ), Cp (47 nF). In this test, the time constant is 94 μs. When observing circumferential dynamic hysteresis loop curves at different frequencies, the time constant should be adjusted accordingly. The differential mode voltage output from the bridge to the instrumentation amplifier is recorded as V. After integration amplification, the obtained output voltage Vch1 is displayed by the oscilloscope ch1 and can be calculated with Eq. (1):

$$V_{ch1} = \frac{G}{RC}\int Vdt \tag{1}$$

where G is the amplification factor of the circuit, then, Eq. (2) is obtained. (a: The radius of the amorphous wire. l: The length of the amorphous wire).

$$V_{ch1} = \frac{G}{RC}\int Vdt = \frac{G}{RC}\cdot\frac{al\mu_0}{3}\left(\int\frac{\partial M_\emptyset}{\partial t}dt\right) = \frac{G\mu_0 al}{3RC}\cdot M_\Phi \tag{2}$$

Substituting the parameters into Eq. (3):

$$M_\Phi = \frac{3RC\cdot V_{ch1}}{G\mu_0 al} \tag{3}$$

Magnetic field intensity is obtained by collecting the voltage at both ends of the resistance Ri by ch2 and dividing the resistance Ri by the current I of the wire. Refer to Eq. (4).

$$H_\varphi = \frac{V_{ch2}}{4\pi aR_i} \tag{4}$$

A Lissajous curve composed of the ch1 and ch2 signals displayed on the oscilloscope is shown in Fig. 5 to obtain a circumferential dynamic hysteresis loop of core wire. The waveform can be saved by the oscilloscope. The saved result is the actual measured voltage value and is not affected by the scale of each axis during display. When the diameter of the tested wire is 120 μm, the length is 2 cm, and the time constant is set to 94 μs, it can be seen from the Lissajous diagram

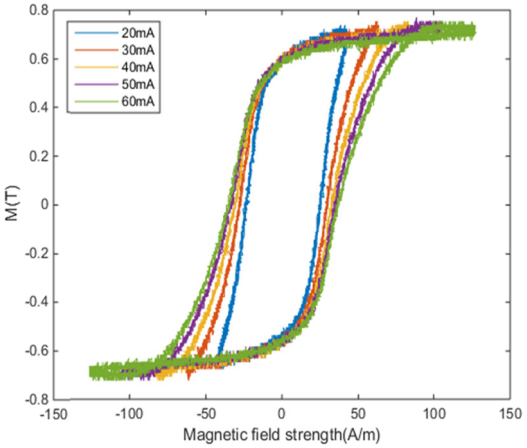

FIGURE 5. Circumferential dynamic hysteresis loop of core wire (120 μm).

in Fig. 5 that the hysteresis loop varies under different current excitations. The better the square ratio of the hysteresis loop is when the excitation current becomes larger, the better the linearity is when the wire is applied to the fluxgate circuit later.

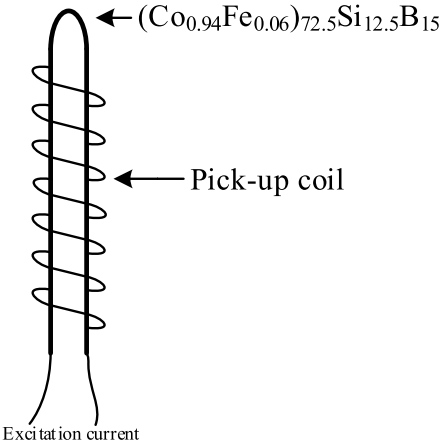

FIGURE 6. Structure of the amorphous wire probe.

The structure of the amorphous wire probe used in the fluxgate circuit is shown in Fig. 6. The probe structure is a U-shaped structure. This structure can effectively reduce the influence of the output bias of the amorphous wire probe under the unidirectional current excitation condition and can effectively reduce the output noise. The diameter of the amorphous wire is 120 μm, the length is 2 cm, the resistance is 2.7 Ω, the diameter of the pick-up coil is 0.1 mm, the outer layer of the amorphous wire is wound with 1200 turns, and the resistance is 112 Ω. The two ends of the amorphous wire are connected with an excitation current signal, and the pick-up coil outputs a voltage signal that responds to the magnetic field information [15]–[17].

III. PRINCIPLE OF ORTHOGONAL FUNDAMENTAL MODE FLUXGATE

The magnetic fluxgate circuit can simultaneously measure the magnetic fields in the X-axis, Y-axis and Z-axis directions.

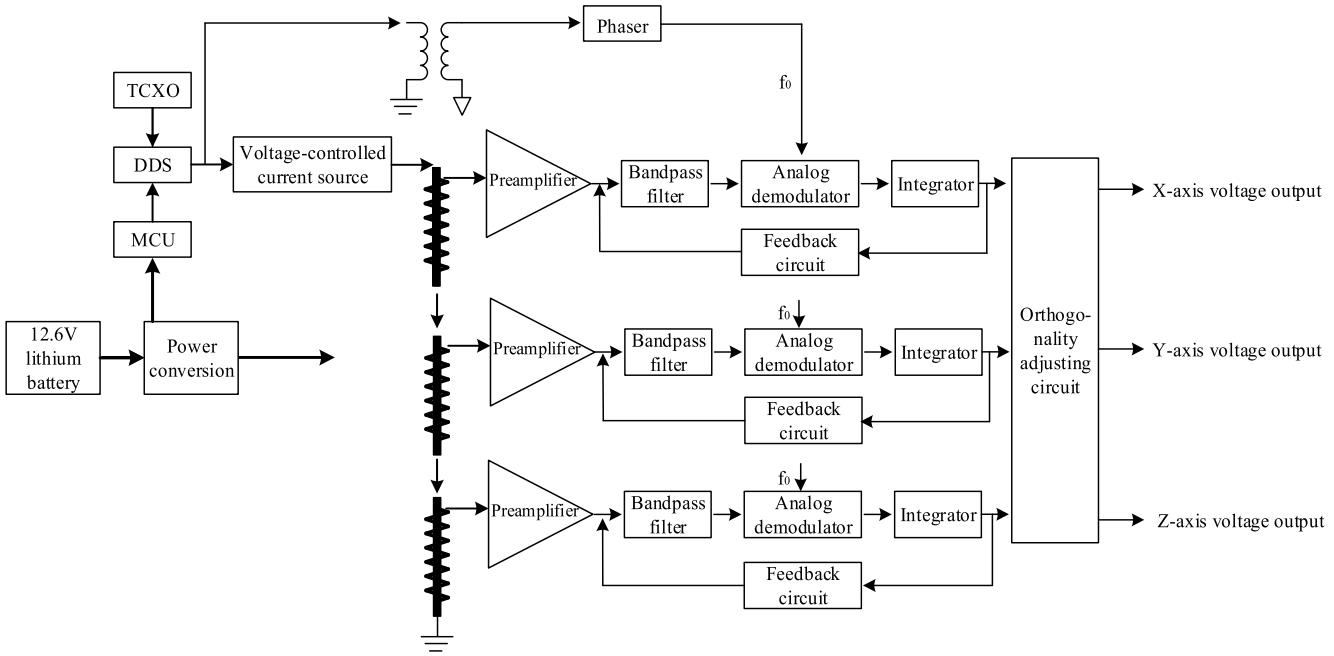

FIGURE 7. Block diagram of the principle of the orthogonal fundamental mode fluxgate circuit.

The circuit principle block diagram is shown in Fig. 7. The magnetic fluxgate circuit is divided into an excitation circuit and a measurement circuit. The MCU (microcontroller unit) in the excitation circuit controls the DDS (direct digital synthesizer) to divide the frequency of the clock signal to generate an excitation voltage signal of 100 kHz. The excitation voltage signal drives the current source to generate an excitation current signal of the corresponding frequency [18], [19]. It is a sinusoidal signal with bias as the excitation current signal of the amorphous wire probe. The probes of the three axes are connected in series to ensure that the amplitude and phase of the excitation current passing through each axis are consistent. The excitation circuit and the measurement circuit are completely isolated. The excitation circuit contains digital circuits, and the measurement circuits are all analog circuits. Isolation can effectively reduce the influence of the excitation circuit on the measurement circuit and is helpful to further reduce the noise of the circuit [20], [21].

The amorphous wire probe modulates the magnetic field signal at a frequency of 100 kHz. A measurement circuit is designed to complete the demodulation of the signal. The measurement circuit includes the preamplifier circuit, bandpass circuit, analog demodulation circuit (AD630 ADI), integration circuit (the time constant is 22 μs.) and feedback circuit which can form a closed-loop measurement system. The feedback resistor adjusts the sensitivity of the circuit by controlling the feedback. The reference signal used in the analog demodulation circuit is provided by the excitation voltage signal in the excitation circuit through the transformer. In the process of demodulation, the phase of the modulation signal must be consistent with the reference phase. Therefore, the phase shift circuit is designed to control the phase of the reference signal. The amplitude of the signal will not change after passing through the phase shift circuit, but the phase can be adjusted within the range of 0 °-180 °. In the design of the three-axis probe, due to the limitation of the manufacturing process, the complete orthogonality of the three axes cannot be completely guaranteed. Therefore, an orthogonality adjusting circuit is added behind the integrator to compensate for the orthogonality of the probe. To reduce the measurement noise of the whole circuit, the magnetic fluxgate circuit is powered by a lithium battery, with a small power ripple and high quality, thus reducing the influence of power noise on the analog circuit.

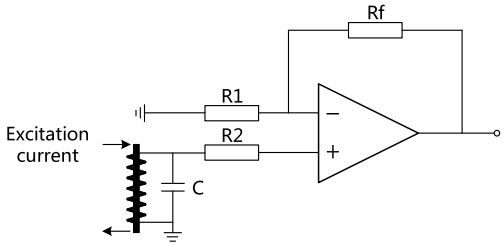

FIGURE 8. Schematic diagram of preamplifier for fluxgate.

The pre-amplifier circuit is shown in Fig. 8. It is designed with the same comparative arithmetic circuit. The resistance value of R1 and R2 is 200 Ω, and the resistance value of Rf is 510 Ω. The pick-up coil is connected in parallel with the capacitor. Thereby improving the signal-to-noise ratio of the output signal of the pick-up coil. The value of the capacitance is related to the inductance of the pick-up coil and the frequency at which resonance occurs.

IV. EXCITATION PARAMETERS OF FLUXGATE AMORPHOUS WIRE PROBE

The output noise of the amorphous wire probe accounts for a large part of the fluxgate noise. The output noise of the probe is directly related to the quality, the magnitude and frequency of the excitation current, and the length of the amorphous wire. Among them, the excitation current has the greatest influence on the output noise of the probe when the wire length is fixed. In addition, the magnitude of the excitation current affects the sensitivity of the sensor probe. The larger the excitation current is, the smaller the sensitivity of the sensor probe and the larger the bias. The output noise of the circuit under different excitation currents is shown in Fig. 9. It can be seen that the output noise of the circuit will increase if the excitation current is too large or too small. After testing groups of excitation currents, the noise output by the probe is smallest under the excitation of a 45 mA bias current and 30 mAp AC amplitude. By testing amorphous wires with different diameters of the same material, the results are basically the same. This picture can help us better choose the appropriate current excitation [22], [23]. Under the same excitation condition, the longer the length of the amorphous wire with the same diameter is, the smaller the noise. However, the size of the magnetic sensor will become larger, which is not conducive to use in engineering measurement.

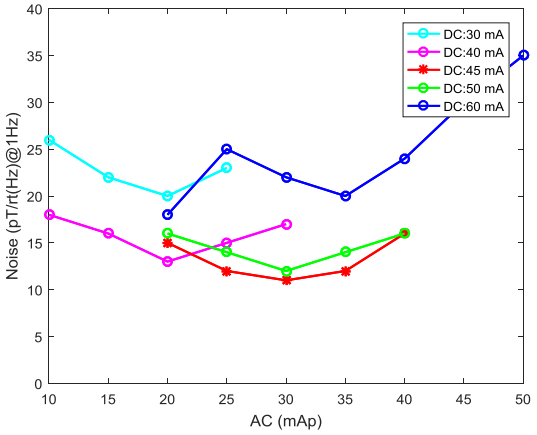

FIGURE 9. Impact of excitation current on output noise.

V. INDICATOR TEST

A. NOISE TEST

Noise performance is a very important indicator of the fluxgate. All testing work is carried out in the underground magnetic shielding room. A noise test diagram is shown in Fig. 10. The probe is placed in a small shielding barrel, and the barrel and fluxgate measurement circuit are placed in a large shielding barrel together, which can reduce the influence of circuit noise on the probe. This test was conducted in a basement to ensure a quiet test environment. When measuring fluxgate noise, the sensor probe and measurement circuit are placed in a high-performance magnetic shielding barrel to ensure a zero magnetic field environment (approximately 1 pT). The output of the fluxgate is connected to a dynamic signal analyzer 35670A (Agilent). The noise test result is derived using MATLAB. The noise observation bandwidth is 31.25 mHz-6.25 Hz and 64 Hz-25.6 kHz. The test results are averaged 20 times. As shown in figure, the noise of the fluxgate is 8.9 pT/rt(Hz)@1 Hz.

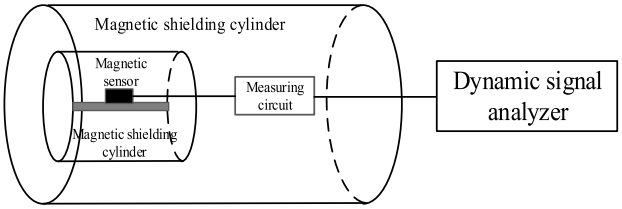

FIGURE 10. Noise test diagram.

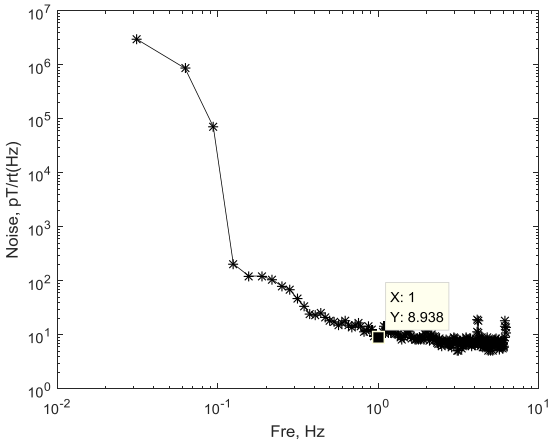

FIGURE 11. Fluxgate output noise spectrum (the noise observation bandwidth is 31.25 mHz-6.25 Hz and the test results are averaged 20 times).

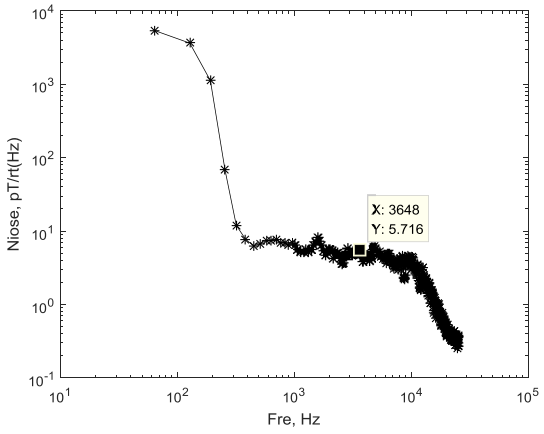

FIGURE 12. Noise floor of fluxgate (the noise observation bandwidth is 64 Hz-25.6 kHz and the test results are averaged 20 times).

B. ORTHOGONALITY TEST

Magnetic field sensors are vector sensors. Due to the electrical characteristics and processing technology of sensor core materials, complete orthogonality cannot be guaranteed between the X-axis, Y-axis and Z-axis. Although

compensation is made in the hardware circuit, an orthogonality error still exists. To test the orthogonality deviation between each axis, the orthogonality test scheme is as follows.

1) Select a space with a uniform magnetic field, and measure the magnetic field intensity B0 in the uniform field area at the center of the magnetic field generator in the magnetic shielding chamber by using an optical pump magnetometer;

2) Rotate the sensor probe randomly in the uniform magnetic field area (the heading angle covers ±180 degrees, the pitch angle covers ±90 degrees, and the roll angle covers ±90 degrees), and continuously record the triaxial output voltage of the sensor, with the sensor output data is recorded being D1;

3) Repeat step 2) to measure the outputs of groups of sensors, and record them as D2, D3, D4, . . .;

4) Based on the measured values D1, D2, D3,. . . , sequentially extract the three-axis orthogonality error angles u1, u2, u3 of the sensor with a digital correction method; u1 angle sequences as u11, u12,. . . , the u2 angle sequences as u21, u22,. . . , and the u3 angle sequences as u31, u32, . . .;

5) Calculate the maximum deviations D(u1), D(u2) and D(u3) of the u1, u2 and u3 angular sequences relative to the mean value of each sequence, as shown in Eq. (5). The maximum deviation of the three represents the maximum deviation of the corrected sensor triaxial orthogonality error angle.

$$D_{max} = max(D(u_1), D(u_2), D(u_3)) \tag{5}$$

The orthogonality error angles of 10 groups of sensors were measured according to the above method, and the measured results are shown in Fig. 13. The three colors represent the X-axis, Y-axis and Z-axis, and the three-axis orthogonality error of the sensors obtained according to the abovementioned test method is 0.04°.

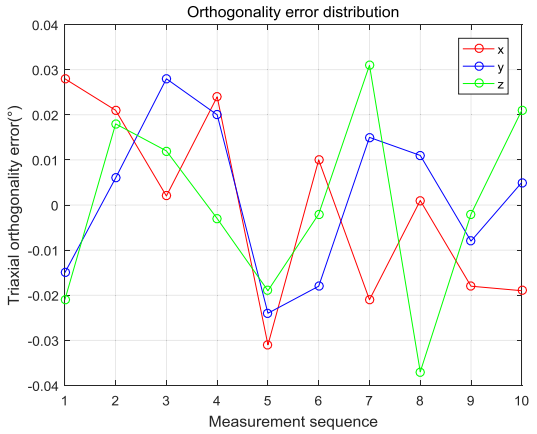

FIGURE 13. Test results of sensor triaxial orthogonality error.

C. WORKING BANDWIDTH TEST

The fluxgate of the orthogonal fundamental mode mechanism can effectively improve the working bandwidth index. The working bandwidth of the fluxgate of the parallel excitation second harmonic method is mostly 3 kHz-6 kHz, and the operating bandwidth of the orthogonal fundamental mode fluxgate is 15 kHz. It has low noise and high bandwidth performance. During the test, the fluxgate is placed in the solenoid, and by supplying alternating current to the solenoid, an alternating magnetic field is generated. The frequency sweep function of the SR785 dynamic signal analyzer is used to test the working bandwidth of the fluxgate. The test results are shown in Fig. 14. The power frequency interference is greater at 50 Hz.

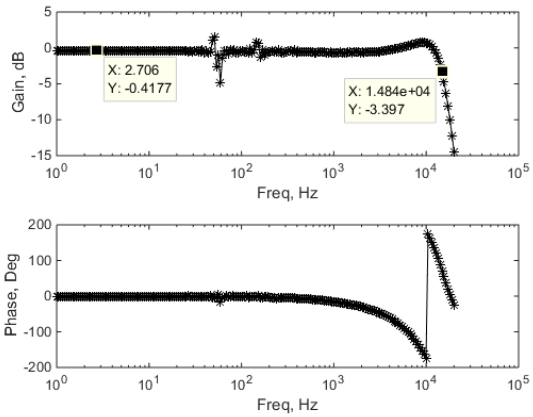

FIGURE 14. Amplitude-frequency characteristics and phase frequency characteristics of the fluxgate sensor circuit.

This article takes the Mag-03 product of Bartington as an example to compare some main parameters.

TABLE 1. Parameter comparison.

Instrument	Noise(@1Hz)	Bandwidth	Dynamic Range
Orthogonal Fundamental Mode Fluxgate	8.9 pT/rt(Hz)	DC-15 kHz	159 dB
Mag-03 (low noise version)	6 pT/rt(Hz)	DC-6 kHz	162.5 dB
Mag-03 (standard version)	10 pT/rt(Hz)	DC-6 kHz	146 dB
Mag-03 (basic version)	20 pT/rt(Hz)	DC-6 kHz	140 dB

VI. CONCLUSION

Different from the parallel excitation second harmonic method, an orthogonal fundamental mode fluxgate is designed in this paper, which can effectively reduce the influence of Barkhausen noise on the fluxgate output noise. After testing, the output noise of the fluxgate is 8.9 pT/rt(Hz)@1 Hz. The operating bandwidth of the orthogonal fundamental mode fluxgate can reach 15 kHz, which is higher than that of the fluxgate with the parallel excitation second harmonic method, providing a direction for designing a high-bandwidth fluxgate. This paper introduces several methods for fluxgate testing. The magnetic field measurement range of the orthogonal fundamental mode fluxgate

is ±100000 nT, the sensitivity is 100 μV/nT, The dynamic range of the fluxgate is 159 dB, and the error of triaxial orthogonality after digital correction is less than 0.04 °, making this fluxgate suitable for use in the field of high-precision magnetic field measurement.

REFERENCES

[1] P. Ripka and M. Janosek, "Advances in magnetic field sensors," *IEEE Sensors J.*, vol. 10, no. 6, pp. 1108–1116, Jun. 2010, doi: 10.1109/JSEN.2010.2043429.

[2] Q. Zhang, W. Li, F. Guo, Z. Yuan, S. Qiao, and Q. Zhang, "Development of a new distributed hybrid seismic and electrical data acquisition station based on system-on-a-programmable-chip technology," *Geosci. Instrum., Methods Data Syst.*, vol. 8, no. 2, pp. 241–249, Sep. 2019, doi: 10.5194/gi-8-241-2019.

[3] U. Topal, H. Can, O. M. Çelik, A. Narman, M. Kamiş, V. Çıtak, D. Çakrak, H. Sözeri, and P. Svec, "Design of fluxgate sensors for different applications from geology to medicine," *J. Supercond. Novel Magn.*, vol. 32, no. 4, pp. 839–844, Apr. 2019, doi: 10.1007/s10948-018-4781-x.

[4] W. Suyuan, Z. Junyun, P. Longxin, and H. Nianning, "0.15 μm GaAs limiter-LNA MMIC base on 248 nm scanner process," *Electron. Packag.*, pp. 39–43, Aug. 2019, doi: 10.16257/356 j.cnki.1681-1070.2019.0811.

[5] P. M. Vetoshko, N. A. Gusev, D. A. Chepurnova, E. V. Samoilova, I. I. Syvorotka, I. M. Syvorotka, A. K. Zvezdin, A. A. Korotaeva, and V. I. Belotelov, "Flux-gate magnetic field sensor based on yttrium iron garnet films for magnetocardiography investigations," *Tech. Phys. Lett.*, vol. 42, no. 8, pp. 860–864, Aug. 2016, doi: 10.1134/S1063785016080289.

[6] S. Qiao, H. Duan, Q. Zhang, Q. Zhang, S. Li, S. Liu, S. Liu, Y. Wang, S. Yan, W. Li, and F. Guo, "Development of high-precision distributed wireless microseismic acquisition stations," *Geosci. Instrum., Methods Data Syst.*, vol. 7, no. 3, pp. 253–263, Sep. 2018, doi: 10.5194/gi-7-253-2018.

[7] E. Paperno, "Suppression of magnetic noise in the fundamental-mode orthogonal fluxgate," *Sens. Actuators A, Phys.*, vol. 116, no. 3, pp. 405–409, Oct. 2004, doi: 10.1016/j.sna.2004.05.011.

[8] M. Butta and I. Coroli, "Low offset Drift–Low-Noise orthogonal fluxgate with synchronized polarity flipping," *IEEE Trans. Magn.*, vol. 53, no. 4, pp. 1–6, Apr. 2017, doi: 10.1109/TMAG.2016.2633484.

[9] M. Butta, I. Sasada, and M. Janosek, "Temperature dependence of offset and sensitivity in orthogonal fluxgate operated in fundamental mode," *IEEE Trans. Magn.*, vol. 48, no. 11, pp. 4103–4106, Nov. 2012, doi: 10.1109/TMAG.2012.2202383.

[10] M. Butta and I. Sasada, "Method for offset suppression in orthogonal fluxgate with annealed wire core," *Sensor Lett.*, vol. 12, no. 8, pp. 1295–1298, Aug. 2014, doi: 10.1166/sl.2014.3311.

[11] M. Butta and M. Janosek, "Very low frequency noise reduction in orthogonal fluxgate," *AIP Adv.*, vol. 8, no. 4, pp. 1–6, 2018.

[12] H. Jing and L. Bin, "Fluxgate sensor based on second harmonic pulse peak-to-peak value law," *Transducer Microsyst. Technol.*, pp. 73–79, Jul. 2007, doi: 10.13873/j.1000-97872007.07.017.

[13] R. Bazinet, A. Jacas, G. A. B. Confalonieri, and M. Vazquez, "A low-noise fundamental-mode orthogonal fluxgate magnetometer," *IEEE Trans. Magn.*, vol. 50, no. 5, pp. 1–3, May 2014, doi: 10.1109/TMAG.2013.2292834.

[14] F. Han, S. Harada, and I. Sasada, "Fluxgate and search coil hybrid: A low-noise wide-band magnetometer," *IEEE Trans. Magn.*, vol. 48, no. 11, pp. 3700–3703, Nov. 2012, doi: 10.1109/TMAG.2012.2196762.

[15] B. B. Narod, "The origin of noise and magnetic hysteresis in crystalline permalloy ring-core fluxgate sensors," *Geosci. Instrum., Methods Data Syst.*, vol. 3, no. 2, pp. 201–210, Sep. 2014.

[16] D. M. Miles, M. Ciurzynski, D. Barona, B. B. Narod, J. R. Bennest, A. Kale, M. Lessard, D. K. Milling, J. Larson, and I. R. Mann, "Low-noise permalloy ring cores for fluxgate magnetometers," *Geosci. Instrum., Methods Data Syst.*, vol. 8, no. 2, pp. 227–240, Sep. 2019, doi: 10.5194/gi-8-227-2019.

[17] D. M. Miles, B. B. Narod, D. K. Milling, I. R. Mann, D. Barona, and G. B. Hospodarsky, "A hybrid fluxgate and search coil magnetometer concept using a racetrack core," *Geosci. Instrum., Methods Data Syst.*, vol. 7, no. 4, pp. 265–276, Oct. 2018, doi: 10.5194/gi-7-265-2018.

[18] P. Baranov, V. Baranova, A. Kolomeytsev, and I. Zatonov, "Drive signal waveform for a fluxgate," *J. Phys. Conf.*, pp. 1–4, Aug. 2018, doi: 10.1088/1742-6596/1065/5/052020.

[19] W. Xiangxin, J. Wenjuan, Y. Yang, Z. Wenjie, and S. Yunbo, "Design of excitation system for fluxgate by sine wave," *Chin. J. Sens. Actuators*, pp. 1887–1892, Dec. 2015, doi: 10.3969/j.issn.1004-1699.2015.12.026.

[20] V. Korepanov and A. Marusenkov, "Flux-gate magnetometers design peculiarities," *Surv. Geophys.*, vol. 33, no. 5, pp. 1059–1079, Sep. 2012, doi: 10.1007/s10712-012-9197-8.

[21] R. N. Setiadi and M. Schilling, "Inductance analyzer based on auto balanced circuit for precision measurement of fluxgate impedance," *Meas. Sci. Technol.*, Feb. 2018, doi: 10.1088/1361-6501/aaae97.

[22] M. Butta, S. Yamashita, and I. Sasada, "Reduction of noise in fundamental mode orthogonal fluxgates by optimization of excitation current," *IEEE Trans. Magn.*, vol. 47, no. 10, pp. 3748–3751, Oct. 2011, doi: 10.1109/TMAG.2011.2152379.

[23] A. Baschirotto, E. Dallago, P. Malcovati, M. Marchesi, and G. Venchi, "From a PCB fluxgate to an integrated micro fluxgate magnetic sensor," in *Proc. Instrum. Meas. Technol. Conf.*, May 2005, pp. 1756–1760, doi: 10.1109/IMTC.2005.1604472.

ZHENZHONG YUAN was born in Weifang, China, in 1994. He received the B.E. degree in measurement and control technology and instrument and the master's degree from the China University of Geosciences (Beijing), Beijing, China, in 2016 and 2019, respectively. His research interests include instrumental science and technology analog circuit design and development, and the development of magnetic field detection instruments.

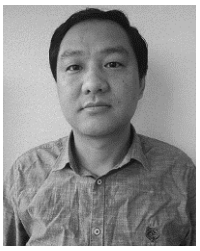

YUXIN ZHANG was born in Wuxi, China, in 1975. He is mainly engaged in technical research in the fields of magnetic measurement and magnetic applications, high-precision data-converters, and geophysical instruments.

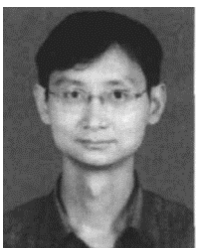

DONG WANG was born in Wuxi, China, in 1971. He received the degree from the Department of Information and Electronics Engineering, Zhejiang University, in 1994. He has been engaged in the design and management of integrated circuits with the China Electronics Technology Group Corporation No. 58 Research Institute.

YINGDAN JIANG was born in Wuxi, China, in 1983. She is mainly engaged in high-speed analog circuit design and research on RF chip transceivers.

RONGHAI GUO received the M.S. degree in communication and information systems from the Army Engineering University of PLA, Nanjing, in 2014. He is an Assistant Engineer. His research interests include signal processing and digital communications.